



# Synthesis and characterization of a series of diphenyldipyrzolylmethane complexes with zinc(II)

Janet L. Shaw\*, Kevin P. Gwaltney, Nikky Keer

Kennesaw State University, Department of Chemistry and Biochemistry, Kennesaw, GA 30144-5591, USA

## ARTICLE INFO

### Article history:

Received 28 July 2008

Received in revised form 17 October 2008

Accepted 23 October 2008

Available online 30 October 2008

### Keywords:

X-ray crystal structures

<sup>1</sup>H NMR

Diphenyldipyrzolylmethane

Zinc(II) complexes

Scorpionates

Chelating ligands

## ABSTRACT

The zinc(II) coordination chemistry of a series of diphenyldipyrzolylmethane ligands was explored using <sup>1</sup>H NMR and single crystal X-ray diffraction. Unsubstituted diphenyldipyrzolylmethane (dpdpm), diphenylbis(3-methylpyrazolyl)methane (dpdp'm), and diphenylbis(3,5-dimethylpyrazolyl)methane (dpdp''m) were reacted with Zn(NO<sub>3</sub>)<sub>2</sub> to afford Zn(dpdpm)(NO<sub>3</sub>)<sub>2</sub>, Zn(dpdp'm)(NO<sub>3</sub>)<sub>2</sub> and Zn(Pz'')<sub>2</sub>(NO<sub>3</sub>)<sub>2</sub> where Pz'' = 3,5-dimethylpyrazole, respectively. All attempts to isolate Zn(dpdp''m)(NO<sub>3</sub>)<sub>2</sub> with the intact dpdp''m ligand were unsuccessful due to decomposition of the ligand. These bidentate ligands support the formation of 1:1 ligand to metal complexes and structurally model the two histidine coordination mode common in zinc proteins.

Published by Elsevier B.V.

## 1. Introduction

Diphenyldipyrzolylmethane is a bidentate, neutral ligand containing two pyrazole moieties available for coordination to metal centers. The sterics and electronics of diphenyldipyrzolylmethane can be adjusted by employing substituted pyrazole moieties during ligand synthesis [1]. This control over ligand design can be used to enforce a desired geometry at a metal center and to tune the reactivity of the metal ligand complex.

In the literature, diphenyldipyrzolylmethane ligands have received relatively little attention compared to their polypyrazolylborate counterparts. In 1993, Shiu et al. isolated three molybdenum complexes with diphenyldipyrzolylmethanes [2], and in 1999 Jordan et al. synthesized cationic palladium(II) alkyl organometallic complexes for use in polymerization catalysis [3]. In addition, Reger et al. used these ligands in 2004 to gain a fundamental understanding of metal cation-π phenyl interactions in complexes with Ag(I) [4]. More recently, attention has shifted to generating diphenyldipyrzolylmethane complexes with the first row transition metals copper(II) and nickel(II). With regards to the copper(II) chemistry, these ligands have been used to mimic histidine coordination which is common in metalloproteins [1a], and have been used in oxalate bridged complexes to study electronic communication between d<sup>9</sup> metal centers [1b]. Most recently, interesting solvato-, vapo-, and thermochromic properties of a series of nickel(II)

diphenyldipyrzolylmethane complexes have been reported by Baho and Zargarian [5].

An investigation of the zinc(II) coordination chemistry of unsubstituted diphenyldipyrzolylmethane (dpdpm), diphenylbis(3-methylpyrazolyl)methane (dpdp'm), and diphenylbis(3,5-dimethylpyrazolyl)methane (dpdp''m) is presented here. Zinc is a biologically relevant metal that serves catalytic and structural roles in more than 300 enzymes [6]. A common amino acid for zinc ligation in these enzymes is histidine, and diphenyldipyrzolylmethane ligands may serve as accurate structural models for the 2 His coordination environment found in carboxypeptidase, thermolysin, and neutral protease [6c]. Here, the reactivity of these ligands and their coordination chemistry with zinc is explored using <sup>1</sup>H NMR and single crystal X-ray diffraction in order to determine if diphenyldipyrzolylmethanes can be used to model the active site structures of zinc containing enzymes.

## 2. Experimental

All syntheses were carried out in air and the reagents and solvents were obtained commercially and used as received. Elemental analysis was performed by Atlantic Microlabs Inc. Fourier transform infrared spectroscopy (FTIR) was performed on powdered solids using a Perkin-Elmer SpectraOne spectrophotometer fitted with a diamond attenuated total reflectance stage. NMR spectra were recorded using a Bruker AVANCE 300 MHz instrument. Melting points (m.p.) were measured using a Mel-Temp<sup>®</sup> instrument. Syntheses of these ligands were reported previously [1a].

\* Corresponding author. Tel.: +1 770 499 3428; fax: +1 770 423 6744.

E-mail address: [jshaw22@kennesaw.edu](mailto:jshaw22@kennesaw.edu) (J.L. Shaw).

Single crystal X-ray diffraction data was collected at the University of Akron. The X-ray intensity data for all compounds were measured at 100 K (Bruker KRYO-FLEX) on a Bruker SMART APEX CCD-based X-ray diffractometer system equipped with a Mo-target X-ray tube ( $\lambda = 0.71073 \text{ \AA}$ ) operated at 2000 W power. Crystals were mounted on a cryoloop using Paratone N-Exxon oil and placed under a stream of nitrogen. The detector was placed at a distance of 5.009 cm from the crystals. Frames were collected with a scan width of  $0.3^\circ$  in  $\omega$ . Analyses of the data sets showed negligible decay during data collection. The data were corrected for absorption with the *SADABS* program. The structures were refined using the Bruker *SHELXTL* Software Package (Version 6.1), and were solved using direct methods until the final anisotropic full-matrix, least squares refinement of  $F^2$  converged [7]. The *PATTERSON* program was used to solve the structure of  $\text{Zn}(\text{dpdp'm})(\text{NO}_3)_2$ .

### 2.1. $\text{Zn}(\text{dpdp'm})(\text{NO}_3)_2$

Dpdp'm (1.26 g, 4.20 mmol) was dissolved in 300 mL of ethanol in a round bottom flask with stir bar. Solid zinc nitrate hexahydrate (1.50 g, 5.04 mmol) was then added to the clear solution. The reaction was allowed to stir overnight at room temperature. Then, the excess solvent was removed via rotary evaporator yielding a white solid. The solid was re-dissolved in dichloromethane and filtered to remove insoluble materials. Slow evaporation of the solvent produced clear, colorless crystals (1.55 g, 76%). X-ray quality crystals were grown from dichloromethane, and crystal data and structure refinement parameters are summarized in Table 1. One of the nitrates is replaced during recrystallization to yield  $\text{Zn}(\text{dpdp'm})(\text{NO}_3)\text{Cl}$  in the solid state.  $^1\text{H}$  NMR (300 MHz,  $\text{CDCl}_3$ ,  $22^\circ\text{C}$ ) 8.17 (d,  $J = 2.1 \text{ Hz}$ , 2H, pyrazole), 7.61 (t,  $J = 7.4 \text{ Hz}$ , 2H, Ph), 7.49 (m, 6H, 4 Ph and 2 pyrazole), 6.62 (d,  $J = 7.2 \text{ Hz}$ , 4H, Ph), 6.57 (t,  $J = 2.5 \text{ Hz}$ , 2H, pyrazole). IR ( $\text{cm}^{-1}$ ): 3394 (w), 3105 (w), 1477 (s), 1450 (m), 1436 (m), 1405 (m),

1383 (m), 1271 (vs), 1253 (m), 1226 (w), 1209 (m), 1198 (m), 1187 (m), 1174 (w), 1163 (w), 1103 (m), 1086 (m), 1066 (s), 1016 (s), 1003 (m), 991 (m), 941 (w), 923 (w), 891 (w), 860 (w), 839 (w), 814 (m), 777 (s), 760 (s), 746 (vs), 699 (s), 657 (m). M.p.  $187\text{--}195^\circ\text{C}$ . Anal. Calc. for  $\text{ZnC}_{19}\text{H}_{16}\text{N}_6\text{O}_6$ : C, 46.58; H, 3.30; N, 17.16. Found: C, 46.52; H, 3.29; N, 17.08%.

### 2.2. $\text{Zn}(\text{dpdp'm})(\text{NO}_3)_2$

Dpdp'm (0.501 g, 1.53 mmol) was dissolved in 200 mL of warm ethanol in a round bottom flask with stir bar. Solid zinc nitrate hexahydrate (0.599 g, 2.01 mmol) was then added to clear the solution. After 2 h of stirring at room temperature a white precipitate began to form. After six hours of stirring the reaction mixture was filtered to isolate the white solid product (0.156 g, 20%). The solid was re-dissolved in dichloromethane and slow evaporation of the solvent produced clear, colorless crystals of X-ray quality. The crystal data and structure refinement parameters are summarized in Table 1.  $^1\text{H}$  NMR (300 MHz,  $\text{CDCl}_3$ ,  $22^\circ\text{C}$ ) 7.61 (t,  $J = 7.4 \text{ Hz}$ , 2H, Ph), 7.49 (t,  $J = 7.7 \text{ Hz}$ , 4H, Ph), 7.35 (d,  $J = 2.7 \text{ Hz}$ , 2H, pyrazole), 6.65 (d,  $J = 5.9 \text{ Hz}$ , 4H, Ph), 6.32 (d,  $J = 2.7 \text{ Hz}$ , 2H, pyrazole), 2.50 (s, 6H, methyl). IR ( $\text{cm}^{-1}$ ): 1527 (w), 1483 (s), 1449 (m), 1382 (m), 1351 (w), 1301 (s), 1280 (vs), 1186 (s), 1076 (s), 1046 (w), 1035 (w), 1009 (s), 937 (w), 914 (w), 886 (m), 862 (m), 835 (w), 809 (m), 793 (m), 779 (m), 765 (s), 749 (s), 713 (s), 693 (s), 656 (m). M.p.  $188\text{--}195^\circ\text{C}$ . Anal. Calc. for  $\text{ZnC}_{21}\text{H}_{20}\text{N}_6\text{O}_6$ : C, 48.70; H, 3.90; N, 16.23. Found: C, 48.30; H, 3.88; N, 16.00%.

### 2.3. $\text{Zn}(\text{Pz''})_2(\text{NO}_3)_2$

This compound was isolated as a decomposition product in the attempt to synthesize  $\text{Zn}(\text{dpdp'm})(\text{NO}_3)_2$ . Dpdp'm (0.500 g, 1.40 mmol) was dissolved in 200 mL of warm ethanol and solid zinc nitrate hexahydrate (0.509 g, 1.71 mmol) was added. The reaction was allowed to stir at reflux overnight. In the morning, the clear, colorless solution was evaporated to dryness using a rotary evaporator. The resulting oil was stored in a vacuum desiccator under reduced pressure for 1 week. NMR analysis of the oil in deuterated chloroform indicated that the dpdp'm ligand had broken apart as evidenced by the single peak at 2.25 ppm indicating equivalent methyl groups on the pyrazole rings. Attempts to separate the mixture of products from this oil for complete analysis were unsuccessful. However, crystals eventually formed in the oil and were analyzed using single crystal X-ray diffraction. The crystal data and structure refinement parameters are summarized in Table 1.

To isolate pure  $\text{Zn}(\text{Pz''})_2(\text{NO}_3)_2$  for complete analysis another synthetic protocol was necessary. The free 3,5-dimethylpyrazole ( $\text{Pz''}$ , 0.505 g, 5.25 mmol) was dissolved in 150 mL of ethanol at room temperature. To this clear solution was added solid zinc nitrate hexahydrate (0.892 g, 3.00 mmol). The reaction was allowed to stir overnight. Then, the excess solvent was removed via rotary evaporation to yield a colorless oil. The oil was placed in a vacuum desiccator for 1 week to dry under reduced pressure. The resulting solid was re-dissolved in dichloromethane and filtered to remove insoluble impurities. Upon slow evaporation of the solvent a light yellow solid was obtained (0.719 g, 72%).  $^1\text{H}$  NMR (300 MHz,  $\text{CD}_3\text{OD}$ ,  $22^\circ\text{C}$ ) 6.14 (s, 2H, pyrazole), 2.31 (s, 12H, methyl). IR ( $\text{cm}^{-1}$ ): 3356 (m), 3252 (m), 3151 (w), 1606 (w), 1576 (m), 1505 (m), 1460 (s), 1414 (m), 1279 (vs), 1176 (m), 1147 (m), 1046 (s), 1004 (s), 812 (m), 806 (m), 756 (w), 744 (w), 656 (m). M.p.  $37\text{--}42^\circ\text{C}$ . Anal. Calc. for  $\text{ZnC}_{10}\text{H}_{16}\text{N}_6\text{O}_6$ : C, 31.47; H, 4.23; N, 22.01. Found: C, 31.60; H, 4.19; N, 21.78%.

**Table 1**  
Selected crystallographic data for all three zinc complexes.

Molecular formula	$\text{ZnC}_{19}\text{H}_{16}\text{N}_6\text{O}_3\text{Cl}$	$\text{ZnC}_{21}\text{H}_{20}\text{N}_6\text{O}_6$	$\text{ZnC}_{10}\text{H}_{16}\text{N}_6\text{O}_6 \cdot \text{CHCl}_3$
Formula weight	463.19	517.82	501.03
Crystal system	triclinic	orthorhombic	monoclinic
Space group	$P\bar{1}$	$P2(1)2(1)2(1)$	$P2(1)/n$
Unit cell dimensions			
<i>a</i> (Å)	10.2143(13)	12.6101(13)	18.043(8)
<i>b</i> (Å)	10.2746(13)	12.8930(13)	12.277(6)
<i>c</i> (Å)	10.4222(13)	13.6505(14)	18.599(8)
$\alpha$ (°)	74.878(2)	90	90
$\beta$ (°)	73.513(2)	90	101.047(7)
$\gamma$ (°)	68.444(2)	90	90
<i>Z</i>	2	4	8
Volume (Å <sup>3</sup> )	960.3(2)	2219.3(4)	4044(3)
Absorption coefficient $\mu_{\text{calc}}$ (mm <sup>−1</sup> )	1.450	1.158	1.651
<i>F</i> (000)	472	1064	2032
$\delta_{\text{calc}}$ (Mg/m <sup>3</sup> )	1.602	1.550	1.646
$\theta$ Range for data collection (°)	2.07–27.00	2.17–28.28	1.44–26.75
Reflections collected/unique	8044/4109	19038/5281	31927/8615
[ <i>R</i> <sub>int</sub> ]	0.0266	0.0597	0.1148
Data/restraints/parameters	4109/0/262	5281/0/309	8615/0/495
Goodness-of-fit (GOF)	1.057	1.001	0.907
Final <i>R</i> indices [ <i>I</i> > 2σ( <i>I</i> )]	<i>R</i> <sub>1</sub> = 0.0330 <i>wR</i> <sub>2</sub> = 0.0753	<i>R</i> <sub>1</sub> = 0.0335 <i>wR</i> <sub>2</sub> = 0.0755	<i>R</i> <sub>1</sub> = 0.0524 <i>wR</i> <sub>2</sub> = 0.1246
<i>R</i> indices (all data)	<i>R</i> <sub>1</sub> = 0.0391 <i>wR</i> <sub>2</sub> = 0.0774	<i>R</i> <sub>1</sub> = 0.0373 <i>wR</i> <sub>2</sub> = 0.0771	<i>R</i> <sub>1</sub> = 0.1304 <i>wR</i> <sub>2</sub> = 0.1346
Largest differences in peak and hole (e Å <sup>−3</sup> )	0.479 and −0.314	1.056 and −0.290	0.539 and −0.924

### 3. Results and discussion

#### 3.1. Synthesis and spectroscopy

The room temperature  $^1\text{H}$  NMR spectra of  $\text{Zn}(\text{dpdpm})(\text{NO}_3)_2$  and  $\text{Zn}(\text{dpdp}'\text{m})(\text{NO}_3)_2$  are very similar so only  $\text{Zn}(\text{dpdpm})(\text{NO}_3)_2$  will be discussed here to avoid redundancy. In the spectrum of the free dpdpm ligand the phenyl protons appear as two sets of multiplets. One multiplet is centered at 7.1 ppm (4H) and the other is centered at 7.4 ppm (6H) [1]. Upon metallation with zinc(II), the phenyl protons of dpdpm separate into three distinct groups. The  $^1\text{H}$  NMR spectrum for  $\text{Zn}(\text{dpdpm})(\text{NO}_3)_2$  and the labeling scheme used for the protons of the ligand are shown in Figs. 1 and 2. Triplets located at 7.6 ppm ( $\text{H}_c$  protons) and 7.5 ppm ( $\text{H}_b$  protons) are shifted slightly downfield relative to the free ligand. The most dramatically shifted phenyl resonance upon metallation is the doublet at 6.6 ppm ( $\text{H}_a$  protons). The significant upfield shift of this resonance results from anisotropic shielding of these protons due to their proximity to the face of the neighboring phenyl ring. This resonance is also broadened relative to the other peaks in the spectrum, and has been shown in the literature to separate into multiple peaks at low temperature due to the constrained orientation of the phenyl rings with respect to each other [3].

Variable temperature  $^1\text{H}$  NMR experiments were also performed on  $\text{Zn}(\text{dpdpm})(\text{NO}_3)_2$  (see [Supplementary Materials](#)). Spectra were recorded in deuterated chloroform spanning the  $-53^\circ\text{C}$  to

$47^\circ\text{C}$  temperature range. At  $47^\circ\text{C}$ , the doublet near 6.6 ppm, assigned to the four phenyl protons labeled  $\text{H}_a$ , sharpens and is much more resolved from the  $\text{H}_4$  protons of the pyrazole rings, as expected, due to rapid interconversion. As the sample is cooled, this doublet broadens and shifts upfield. At  $-13^\circ\text{C}$ , this peak becomes a featureless broad resonance spanning one ppm, superimposed with the peak from the  $\text{H}_4$  protons of the pyrazole rings. By  $-53^\circ\text{C}$ , this peak has narrowed significantly and shifted to 6.0 ppm. The depleted integration (2H), as well as significant changes in the resonances spanning 7.3–8.0 ppm, confirms that the four protons labeled  $\text{H}_a$  are not equivalent at  $-53^\circ\text{C}$ . These variable temperature  $^1\text{H}$  NMR results follow trends observed in the literature for similar metal complexes with diphenyldipyrzolylmethane ligands. Both the room temperature and variable temperature  $^1\text{H}$  NMR spectra support the solution state structure of  $\text{Zn}(\text{dpdpm})(\text{NO}_3)_2$ .

A variety of reaction conditions were employed in attempts to isolate  $\text{Zn}(\text{dpdp}'\text{m})(\text{NO}_3)_2$ . Several dry solvents were tested under anaerobic conditions, and different metal starting salts such as anhydrous zinc chloride and zinc acetate were also employed. However, all attempts to isolate  $\text{Zn}(\text{dpdp}'\text{m})(\text{NO}_3)_2$  were unsuccessful due to decomposition of the ligand.

Room temperature  $^1\text{H}$  NMR was used to study the decomposition of dpdp'm and the subsequent formation of  $\text{Zn}(\text{Pz}'')_2(\text{NO}_3)_2$ . To begin, dpdp'm was dissolved in d-MeOH and a baseline spectrum was recorded. Some of the ligand remained undissolved in the NMR tube, but heat was not applied at this point in the experiment. Then, solid  $\text{Zn}(\text{NO}_3)_2 \cdot 6\text{H}_2\text{O}$  was added and spectra were recorded periodically over the next 24 h. To observe the decomposition of dpdp'm it is easiest to follow the methyl resonances of the intact ligand at 2.08 and 1.45 ppm because, upon ligand decomposition, these two peaks are replaced by a single resonance which appears slightly downfield. This new singlet results from the six hydrogen atoms of the magnetically equivalent methyl groups of 3,5-dimethylpyrazole ( $\text{Pz}''$ ).

Fig. 3 shows representative  $^1\text{H}$  NMR spectra from this experiment. The first indication of ligand decomposition occurs after 2.5 h with a tiny peak growing in at 2.1 ppm. After about 24 hours at room temperature the ratio of the methyl peaks for  $\text{Pz}''$  and intact dpdp'm is 1:2:2, respectively. At this point the contents of the NMR tube were warmed on a hotplate for 15 min. Heating increased the solubility of dpdp'm, and a spectrum was recorded immediately following which showed that the decomposition

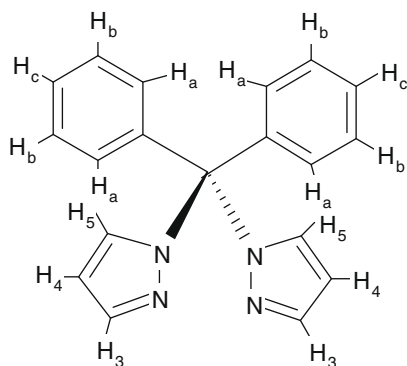


Fig. 1. Labeling scheme of diphenyldipyrzolylmethane used for  $^1\text{H}$  NMR.

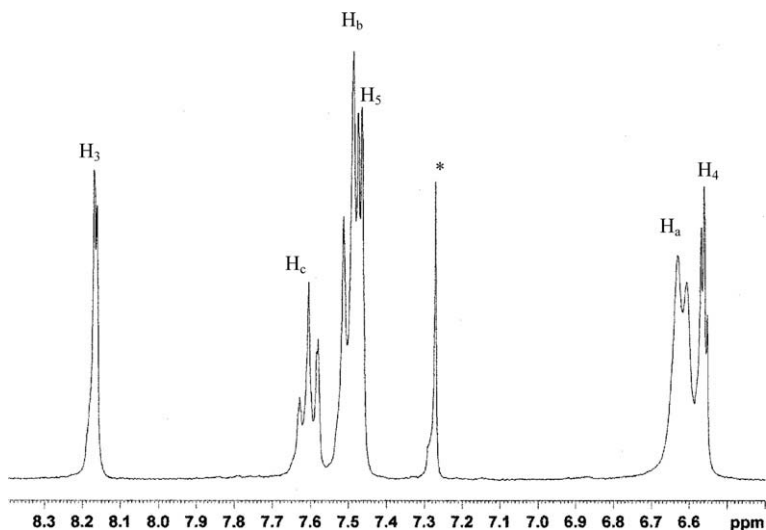


Fig. 2. Room temperature  $^1\text{H}$  NMR spectrum for  $\text{Zn}(\text{dpdpm})(\text{NO}_3)_2$  run in  $\text{CDCl}_3$ .

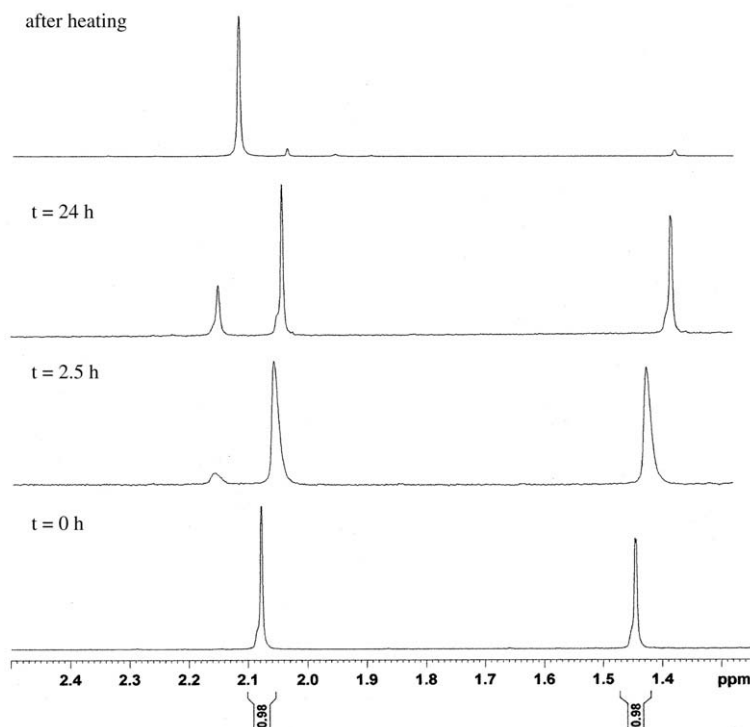


Fig. 3. Selected room temperature  $^1\text{H}$  NMR spectra from the dpdp'm decomposition study (performed in d-MeOH).

product had dramatically increased in concentration giving a ratio of 19:1:1 for the methyl peaks of Pz'' and dpdp'm. An upfield shift of all three peaks is also observed in the spectrum following heating.

Decomposition of similar pyrazole based ligands upon reaction with metal salts has been reported in the literature [8]. The proposed mechanism involves metal-mediated hydrolysis of the pyrazole nitrogen-X bond where X may be boron, as is the case with pyrazolylborates, or carbon, as is the case in this report [1a]. For the pyrazolylborates substitution at the 5-position of the pyrazole ring often helps protect B–N bonds from hydrolysis [9]. However, here the addition of a methyl substituent at the 5-position of the pyrazole ring decreases the stability of dpdp'm in the presence of  $\text{Zn}(\text{NO}_3)_2$  relative to the 3-methylated dpdp'm ligand for which a zinc complex was obtained. This trend in reactivity was also reported previously in a paper employing  $\text{Cu}(\text{NO}_3)_2$  [1a]. Thus far, only molybdenum carbonyl has been successfully incorporated into a complex with the intact dpdp'm ligand according to the literature [2].

### 3.2. X-ray crystallography

Suitable crystals for single crystal X-ray diffraction studies were obtained for each of the zinc complexes. Crystallographic data are located in Table 1, and selected bond distances and angles are provided in Table 2. Figs. 4–6 contain perspective views of the three zinc complexes.

Dpdp'm forms a 1:1 metal-to-ligand complex with zinc(II) in the solid state. One of the two ligated nitrates in the  $\text{Zn}(\text{dpdp'm})(\text{NO}_3)_2$  complex (supported by elemental analysis) is replaced by a chloride during recrystallization in methylene chloride to yield  $\text{Zn}(\text{dpdp'm})(\text{NO}_3)\text{Cl}$  (Fig. 4). Because of the flexibility in nitrate coordination, and the fact that nitrate is isoelectronic with bicarbonate which is important in the catalytic cycle of carbonic anhydrase, a way to quantitate the denticity of metal bound nitrates is commonly used in the literature. The difference between the two

Table 2

Selected bond angles ( $^\circ$ ) and lengths ( $\text{\AA}$ ) for all three zinc complexes.

<b><math>\text{ZnC}_{19}\text{H}_{16}\text{N}_5\text{O}_3\text{Cl}</math></b>			
Zn–O1	2.0016(16)	O1–Zn–N2	103.07(7)
Zn–O2	2.4768(17)	O2–Zn–N2	154.36(6)
Zn–N2	2.0417(18)	O1–Zn–N4	129.13(7)
Zn–N4	2.0179(18)	O2–Zn–N4	92.63(6)
Zn–Cl	2.2070(6)	O1–Zn–O2	56.57(6)
		N2–Zn–N4	89.85(7)
		O1–Zn–Cl	108.68(5)
		O2–Zn–Cl	94.89(4)
		N2–Zn–Cl	107.40(5)
		N4–Zn–Cl	113.83(5)
<b><math>\text{ZnC}_{21}\text{H}_{20}\text{N}_6\text{O}_6</math></b>			
Zn–O1	2.4730(18)	O2–Zn–N2	104.91(7)
Zn–O2	2.005(16)	O4–Zn–N2	188.04(7)
Zn–O4	1.9605(17)	O2–Zn–N4	125.56(7)
Zn–N2	2.0189(18)	O4–Zn–N4	122.40(7)
Zn–N4	1.9959(18)	O1–Zn–O4	88.18(7)
		O2–Zn–O4	96.76(7)
		O1–Zn–N2	150.99(7)
		O1–Zn–N4	86.01(7)
		O1–Zn–O2	56.67(6)
		N2–Zn–N4	89.37(7)
<b><math>\text{ZnC}_{10}\text{H}_{16}\text{N}_6\text{O}_6 \cdot \text{CHCl}_3</math></b>			
Zn1–O1	2.064(4)	O1–Zn1–N1	104.72(17)
Zn1–O3	2.553(4)	O4–Zn1–N1	154.49(15)
Zn1–O4	2.427(4)	O5–Zn1–N1	98.77(16)
Zn1–O5	2.055(4)	O1–Zn1–N3	98.83(16)
Zn1–N1	2.009(4)	O4–Zn1–N3	93.29(15)
Zn1–N3	1.995(4)	O5–Zn1–N3	116.31(16)
		O1–Zn1–O4	88.06(14)
		O1–Zn1–O5	129.83(15)
		O4–Zn1–O5	57.05(13)
		N1–Zn1–N3	106.11(18)
		O7–Zn2–N5	108.49(17)
Zn2–O7	2.031(4)	O7–Zn2–N7	104.53(16)
Zn2–O8	2.582(4)	O10–Zn2–N5	136.01(16)
Zn2–O10	1.993(4)	O10–Zn2–N7	97.38(17)
Zn2–N5	1.961(4)	O10–Zn2–O7	101.58(15)
Zn2–N7	2.009(4)	N5–Zn2–N7	105.051(19)



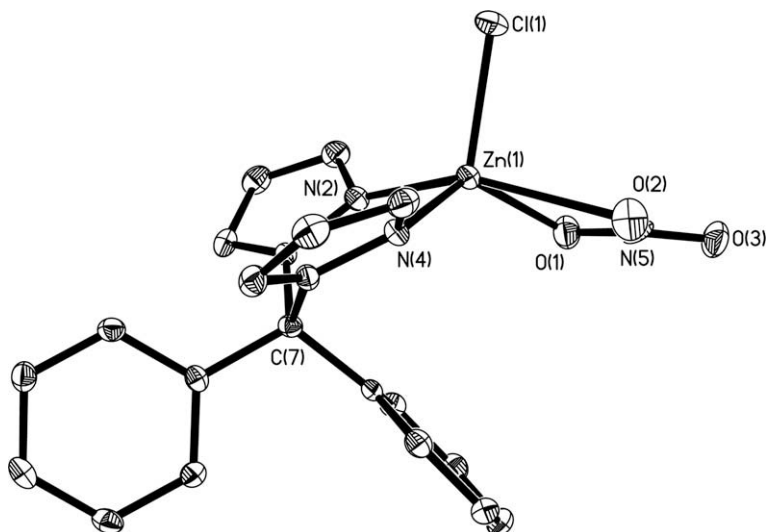


Fig. 4. Structure of  $\text{Zn}(\text{dpdpm})(\text{NO}_3)\text{Cl}$  with 50% thermal ellipsoids and hydrogen atoms omitted for clarity.

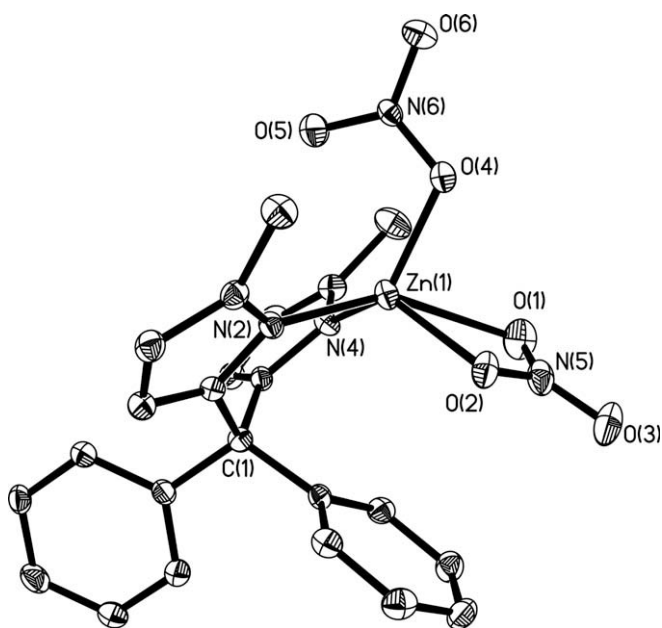


Fig. 5. Structure of  $\text{Zn}(\text{dpdpm})(\text{NO}_3)_2$  with 50% thermal ellipsoids and hydrogen atoms omitted for clarity.

$\text{M}-\text{O}_{\text{NO}_3}$  distances ( $\Delta d$ ) and the difference between the two  $\text{M}-\text{O}-\text{N}$  angles ( $\Delta\theta$ ) are used to classify nitrate denticity ( $\Delta d < 0.3 \text{ \AA}$  and  $\Delta\theta < 14^\circ$  for bidentate;  $0.3 < \Delta d < 0.6 \text{ \AA}$  and  $14 < \Delta\theta < 28^\circ$  for anisodentate;  $\Delta d > 0.6 \text{ \AA}$  and  $\Delta\theta > 28^\circ$  for monodentate) [6c]. Using this method, the binding mode of the nitrate in  $\text{Zn}(\text{dpdpm})(\text{NO}_3)\text{Cl}$  is best described as anisobidentate ( $\Delta d = 0.48 \text{ \AA}$  and  $\Delta\theta = 21.37^\circ$ ).

Therefore, the zinc center in  $\text{Zn}(\text{dpdpm})(\text{NO}_3)\text{Cl}$  is five coordinate, and with  $\tau = 0.42$  the geometry at the metal is best described as distorted square pyramidal [10]. The chloride is best treated as the axial ligand in this geometry, leaving the anisobidentate nitrate and the chelating dpdpm to complete the basal plane (Fig. 4). The small bite angle of the nitrate ( $\sim 56^\circ$ ) leads to significant distortion in the basal plane, and the zinc ion is displaced  $0.60 \text{ \AA}$  from the mean plane generated by N2–N4–O2–O1 towards the axial chloride. The chloride leans slightly off-axis away from the dpdpm ligand with Cl–Zn–N2 and Cl–Zn–N4 angles of around  $107^\circ$  and  $114^\circ$ , respectively. The Zn–N<sub>pz</sub> and Zn–Cl bond lengths are close to those found in similar complexes [11].

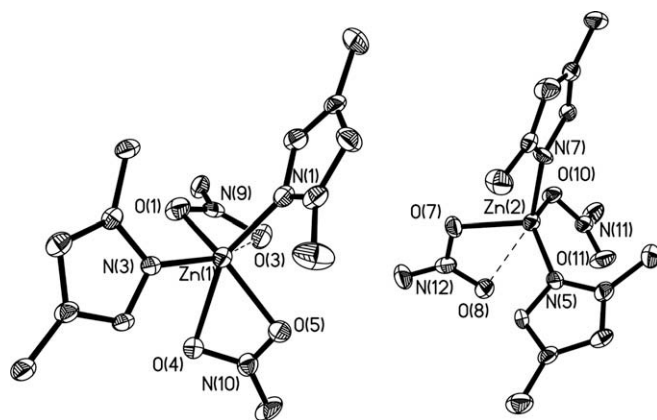


Fig. 6. Structure of  $\text{Zn}(\text{Pz}')_2(\text{NO}_3)_2$  with 50% thermal ellipsoids. Chloroform molecules and hydrogen atoms omitted for clarity.

The six-membered ring formed by the chelating dpdpm ligand is in an approximate boat conformation as indicated by the  $169.03^\circ$  angle between the N–Zn–N and the N–N–N–N planes (Table 3) [3]. One phenyl ring of dpdpm points towards the zinc, and the closest Zn–C<sub>ph</sub> interactions are at  $3.37$  and  $3.89 \text{ \AA}$ . As stated in the literature, these M–C<sub>ph</sub> interactions are most likely due to steric congestion around the quaternary carbon of the ligand which results in constrained ligand geometry; rather than metal cation– $\pi$  interactions [4]. The phenyl rings of dpdpm may help the isolation of 1:1 metal-to-ligand complexes with zinc(II) in the solid state; whereas bis-(pyrazolyl)alkane derivatives and tris-(pyrazolyl)methane ligands have been shown to produce 1:2 complexes upon reaction with  $\text{Zn}(\text{NO}_3)_2$  in the literature [12].

The X-ray crystal structure of  $\text{Zn}(\text{dpdpm})(\text{NO}_3)_2$  (Fig. 5) compares nicely to that of  $\text{Zn}(\text{dpdpm})(\text{NO}_3)\text{Cl}$  with only subtle differ-

Table 3  
Angles generated by selected planes.

	$\text{Zn}(\text{dpdpm})(\text{NO}_3)\text{Cl}$	$\text{Zn}(\text{dpdpm})(\text{NO}_3)_2$
N–Zn–N/N–N–N–N	169.03	155.62
N–C–N/N–N–N–N	127.63	130.58
Pz/pz	131.02	135.82
N–Zn–N/pz	27.57/23.63	32.36/30.06
N–N–N/pz	27.37/22.02	27.06/17.23

ences owing to the 3-methyl substituents of the pyrazole moieties. One nitrate in  $\text{Zn}(\text{dpdp}'\text{m})(\text{NO}_3)_2$  is bound to zinc in an anisobidentate fashion ( $0.47 \text{ \AA}$  and  $20.42^\circ$ ) while the other is clearly monodentate ( $0.79 \text{ \AA}$  and  $36.49^\circ$ ) based on the calculated values for  $\Delta d$  and  $\Delta\theta$ .

Therefore, the zinc center is five coordinate, and with  $\tau = 0.42$  the geometry of  $\text{Zn}(\text{dpdp}'\text{m})(\text{NO}_3)_2$  is also distorted square pyramidal. The monodentate nitrate is best treated as the axial ligand in this complex, leaving the anisobidentate nitrate and  $\text{dpdp}'\text{m}$  to complete the basal plane. The small bite angle of the anisobidentate nitrate ( $\sim 57^\circ$ ) leads to significant distortion in the basal plane with angles deviating significantly from the ideal  $90^\circ$ . The zinc ion is displaced  $0.66 \text{ \AA}$  from the mean plane generated by  $\text{N}2\text{--N}4\text{--O}2\text{--O}1$  towards the axial nitrate. The axial nitrate is leaning off-axis away from the  $\text{dpdp}'\text{m}$  ligand with  $\text{O}4\text{--Zn--N}2$  and  $\text{O}4\text{--Zn--N}4$  angles of around  $118^\circ$  and  $122^\circ$ , respectively. This deviation is more pronounced than in  $\text{Zn}(\text{dpdp}'\text{m})(\text{NO}_3)\text{Cl}$  due to steric interactions with the 3-methyl substituents of the pyrazole rings.

One phenyl ring of  $\text{dpdp}'\text{m}$  points towards the zinc center, and the closest metal– $\text{C}_{\text{ph}}$  interactions are at  $3.25$  and  $3.61 \text{ \AA}$ . The boat conformation formed by the chelating  $\text{dpdp}'\text{m}$  ligand is more pronounced in  $\text{Zn}(\text{dpdp}'\text{m})(\text{NO}_3)_2$  relative to  $\text{Zn}(\text{dpdp}'\text{m})(\text{NO}_3)\text{Cl}$  with a smaller angle between the  $\text{N--Zn--N}$  and  $\text{N--N--N}$  planes ( $155.62^\circ$  versus  $169.03^\circ$ ). This is due to steric crowding associated with the methyl substituents on the pyrazole rings.

The average  $\text{Zn--N}_{\text{pz}}$  bond length of  $2.02 \text{ \AA}$  in  $\text{Zn}(\text{dpdp}'\text{m})(\text{NO}_3)_2$  and  $\text{Zn}(\text{dpdp}'\text{m})(\text{NO}_3)\text{Cl}$  compares nicely with the  $\text{Zn--N}_{\text{His}}$  bond length of around  $2.1 \text{ \AA}$  found in many zinc metalloproteins [13]. For example, in carboxypeptidase A the  $\text{Zn--N}_{\text{His}}$  bond lengths are  $2.00$  and  $2.08 \text{ \AA}$  [14]. In addition, the average bond lengths of the anisobidentate nitrates of  $2.00$  and  $2.48 \text{ \AA}$  from these two complexes are close to the observed  $\text{Zn--O}_{\text{Glu}}$  bond distances of around  $2.1$  and  $2.5 \text{ \AA}$  in neutral protease from *Bacillus cereus* [15]. The  $\text{Zn--N}_{\text{pz}}$  and  $\text{Zn--O}_{\text{mono/aniso}}$  bond lengths are also close to those seen in similar coordination complexes such as  $\text{Zn}(\text{acetate})_2(2,9\text{-dimethyl-}o\text{-phenanthroline})\cdot 3\text{H}_2\text{O}$  ( $\text{Zn--N} = 2.06$  and  $2.09 \text{ \AA}$ ;  $\text{Zn--O}_{\text{mono}} = 1.91$ ,  $\text{Zn--O}_{\text{aniso}} = 2.08$  and  $2.36 \text{ \AA}$ ) [14].

Finally,  $\text{Zn}(\text{Pz}'')_2(\text{NO}_3)_2$  actually crystallizes with two slightly different zinc ions and two chloroform solvent molecules in the unit cell (Fig. 6). The coordination sphere of each zinc ion differs based on the binding modes of the nitrates. Both nitrates surrounding  $\text{Zn}(1)$  are best described as anisobidentate based on the calculated values for  $\Delta d$  and  $\Delta\theta$  ( $0.37 \text{ \AA}/22.68^\circ$  and  $0.49 \text{ \AA}/17.10^\circ$ ). The nitrates surrounding  $\text{Zn}(2)$  each bind differently. One nitrate is bound in an anisobidentate fashion ( $0.55 \text{ \AA}/25.40^\circ$ ), while the other nitrate is clearly bound in a monodentate fashion ( $0.78 \text{ \AA}/34.93^\circ$ ). Carrano et al. reported on a similar case where two crystal isomorphs of the complex  $\text{Zn}(\text{NO}_3)_2(\text{L}1\text{OH})$  were isolated (where  $\text{L}1\text{OH} = 2\text{-hydroxy-3-}t\text{-butyl-methylphenyl} \text{bis}(3,5\text{-dimethylpyrazolyl})\text{methane}$ ) [8e]. In one form both nitrates were bound in an anisobidentate fashion while in the other form they were both bound in a monodentate fashion. Crystal packing forces were used to explain the difference in nitrate binding mode [8e].

Compared to  $\text{Cu}(\text{Pz}'')_3(\text{NO}_3)_2$  [1a], the zinc complex  $\text{Zn}(\text{Pz}'')_2(\text{NO}_3)_2$  has the same average  $\text{M--N}_{\text{pz}}$  distances of  $2.00 \text{ \AA}$ . The bond lengths for the anisobidentate nitrates are also very similar in these two complexes with  $\text{M--O}_{\text{aniso}}$  distances around  $2.0$  and  $2.5 \text{ \AA}$ . However, the bond lengths for the monodentate nitrates do vary significantly ( $\text{M--O}_{\text{mono}} = 1.99 \text{ \AA}$  and  $2.31 \text{ \AA}$  for zinc and copper, respectively). The higher coordination number around copper relative to zinc in these two complexes may be responsible for this longer bond observed in  $\text{Cu}(\text{Pz}'')_3(\text{NO}_3)_2$ .  $\text{Zn}(\text{acetate})_2(\text{imidazole})_2$  also has similar  $\text{Zn--N}$  ( $2.00 \text{ \AA}$ ) and  $\text{Zn--O}$  bond lengths ( $\text{Zn--O}_{\text{mono}} = 1.96 \text{ \AA}$ ,  $\text{Zn--O}_{\text{aniso}} = 1.99$  and  $2.66 \text{ \AA}$ ) with the monodentate nitrate at a distance similar to that observed for  $\text{Zn}(\text{Pz}'')_2(\text{NO}_3)_2$  [14].

## 4. Conclusions

Three new zinc(II) complexes were synthesized using diphenyldipyrzolylmethane ligands.  $\text{Zn}(\text{dpdp}'\text{m})(\text{NO}_3)\text{Cl}$  and  $\text{Zn}(\text{dpdp}'\text{m})(\text{NO}_3)_2$  were isolated as 1:1 metal to ligand complexes in the solid state. Attempts to isolate  $\text{Zn}(\text{dpdp}'\text{m})(\text{NO}_3)_2$  were unsuccessful due to decomposition of the  $\text{dpdp}'\text{m}$  ligand in the presence of metal. Instead,  $\text{Zn}(\text{Pz}'')_2(\text{NO}_3)_2$  was obtained and characterized. Future work will include a detailed NMR study of the conditions leading to  $\text{dpdp}'\text{m}$  ligand decomposition. We also plan to continue exploring the metal chemistry of diphenyldipyrzolylmethane ligands in hopes of synthesizing models of protein active sites.

## Acknowledgements

J.L.S. would like to thank Dr. Chris Ziegler at the University of Akron for graciously collecting the single crystal X-ray diffraction data and the Center for Excellence in Teaching and Learning Incentive Grant at Kennesaw State University for financial support. We wish to also acknowledge NSF Grant CHE-0116041 for funds used to purchase the Bruker-Nonius diffractometer.

## Appendix A. Supplementary material

CCDC 690653, 690654 and 690655 contain the supplementary crystallographic data for this paper. These data can be obtained free of charge from The Cambridge Crystallographic Data Centre via [www.ccdc.cam.ac.uk/data\\_request/cif](http://www.ccdc.cam.ac.uk/data_request/cif). Supplementary data associated with this article can be found, in the online version, at [doi:10.1016/j.ica.2008.10.024](https://doi.org/10.1016/j.ica.2008.10.024).

## References

- [1] (a) J.L. Shaw, T. Cardon, G. Lorigan, C.J. Ziegler, *Eur. J. Inorg. Chem.* (2004) 1073; (b) J.L. Shaw, G.T. Yee, G.W. Wang, D.E. Benson, C. Gokdemir, C.J. Ziegler, *Inorg. Chem.* 44 (2005) 5060.
- [2] K. Shiu, L. Yeh, S. Peng, M. Cheng, *J. Organomet. Chem.* 460 (1993) 203.
- [3] S. Tsuji, D.C. Swenson, R.F. Jordan, *Organometallics* 18 (1999) 4758.
- [4] D.L. Reger, J.R. Gardinier, M.D. Smith, *Inorg. Chem.* 43 (2004) 3825.
- [5] (a) N. Baho, D. Zargarian, *Inorg. Chem.* 46 (2007) 299; (b) N. Baho, D. Zargarian, *Inorg. Chem.* 46 (2007) 7621.
- [6] (a) R.R. Crichton, *Biological Inorganic Chemistry*, Elsevier, Amsterdam, The Netherlands, 2008; (b) H.B. Kraatz, N. Metzler-Nolte, *Concepts and Models in Bioinorganic Chemistry*, Wiley-VCH Verlag GmbH & Co., KGaA, Weinheim, 2006; (c) G. Parkin, *Chem. Rev.* 104 (2004) 699; (d) H. Vahrenkamp, *Acc. Chem. Res.* 32 (1999) 589.
- [7] G.M. Sheldrick, *SHELXTL, Crystallographic Software Package*, Version 6.10, Bruker-AXS, Madison, WI, 2000.
- [8] (a) J.L. Schneider, V.G. Young, W.B. Tolman, *Inorg. Chem.* 40 (2001) 165; (b) C.H. Dungan, W. Maringgele, A. Meller, K. Niedenzu, H. Nöth, J. Serwatowska, *Inorg. Chem.* 30 (1991) 4799; (c) R. Alsasser, S. Trofimenko, A. Looney, G. Parkin, H. Vahrenkamp, *Inorg. Chem.* 30 (1991) 4098; (d) C. Titze, J. Hermann, H. Vahrenkamp, *Chem. Ber.* 128 (1995) 1095; (e) Z. Shirin, B.S. Hammes, C.R. Warthen, C.J. Carrano, *J. Chem. Crystallogr.* 33 (2003) 431; (f) S. Bieller, A. Haghir, M. Bolte, J.W. Bats, M. Wagner, H. Lerner, *Inorg. Chim. Acta* 359 (2006) 1559.
- [9] M. Ruf, H. Vahrenkamp, *Inorg. Chem.* 35 (1996) 6571.
- [10] A.W. Addison, T.N. Rao, J. Reedijk, J. van Rijn, G.C. Verschoor, *J. Chem. Soc., Dalton Trans.* (1984) 1349.
- [11] E.T. Papish, M.T. Taylor, F.E. Jernigan, M.J. Rodig, R.R. Shawhan, G.P.A. Yap, F.A. Jove, *Inorg. Chem.* 45 (2006) 2242 (and references therein).
- [12] (a) M.F. Mahon, J. McGinley, K.C. Molloy, *Inorg. Chim. Acta* 355 (2003) 368; (b) T. Astley, J.M. Gulbis, M.A. Hitchman, E.R.T. Tiekink, *J. Chem. Soc., Dalton Trans.* (1993) 509.
- [13] W.N. Lipscomb, N. Sträter, *Chem. Rev.* (1996) 2375.
- [14] H. Feinberg, H.M. Greenblatt, V. Behar, C. Gilon, S. Cohen, A. Bino, G. Shoham, *Acta Cryst. D51* (1995) 428.
- [15] W. Stark, R.A. Paupit, K.S. Wilson, J.N. Jansonius, *Eur. J. Biochem.* 207 (1993) 781.